Nicole Donato
Christopher Aul
Eric Petersen

Department of Mechanical Engineering,
Texas A&M University,
College Station, TX 77843

Christopher Zinner
Department of Mechanical, Materials and
Aerospace Engineering,
University of Central Florida,
Orlando, FL 32816

Henry Curran
School of Chemistry,
National University of Ireland Galway,
Galway, Ireland

Gilles Bourque
Rolls-Royce Canada,
Montreal, Canada H8T 1A2

Ignition and Oxidation of 50/50 Butane Isomer Blends

One of the alkanes found within gaseous fuel blends of interest to gas turbine applications is butane. There are two structural isomers of butane, normal butane and isobutane, and the combustion characteristics of either isomer are not well known. Of particular interest to this work are mixtures of n-butane and isobutane. A shock-tube experiment was performed to produce important ignition-delay-time data for these binary butane isomer mixtures, which are not currently well studied, with emphasis on 50-50 blends of the two isomers. These data represent the most extensive shock-tube results to date for mixtures of n-butane and isobutane. Ignition within the shock tube was determined from the sharp pressure rise measured at the end wall, which is characteristic of such exothermic reactions. Both experimental and kinetics modeling results are presented for a wide range of stoichiometries ($\phi = 0.3 - 2.0$), temperatures (1056–1598 K), and pressures (1–21 atm). The results of this work serve as a validation for the current chemical kinetics model. Correlations in the form of Arrhenius-type expressions are presented, which agree well with both the experimental results and the kinetics modeling. The results of an ignition-delay-time sensitivity analysis are provided, and key reactions are identified. The data from this study are compared with the modeling results of 100% normal butane and 100% isobutane. The 50/50 mixture of n-butane and isobutane was shown to be more readily ignitable than 100% isobutane but reacts slower than 100% n-butane only for the richer mixtures. There was little difference in ignition time between the lean mixtures. [DOI: 10.1115/1.3204654]

1 Introduction

Fuel-flexible gas turbines are of interest to the power generation industry due to the increasing level of variation in hydrocarbon fuel composition. It is very important that the combustion chemistry is well understood to avoid problems in the combustion system such as flashback, blowoff, instabilities, and autoignition [1,2]. Thus, there is a need to perform experiments to validate the detailed chemistry mechanisms for various higher order hydrocarbons. The focus of this paper is on the chemistry of a butane fuel blend comprised of 50% *n*-butane with 50% isobutane in air. Although this blend may not be a practical fuel for use on its own, its chemistry is a fundamental part of other hydrocarbon fuels such as liquefied natural gas (LNG) and refinery fuels used in industrial applications. Most importantly, the present work provides the validation of chemistry models at practical engine conditions.

Previous work has shown that butane isomers have different combustion characteristics. Structurally, *n*-butane is the unbranched alkane with four carbon atoms, while isobutane, also known as 2-methylpropane, is the branched structure of butane, as seen in Fig. 1 [3]. Although *n*-butane and isobutane have many similar properties, for example, molar mass, they also have dissimilar properties such as boiling point and autoignition temperature. Normal butane has been shown to be more readily ignitable than isobutane [4].

Butane, like many other complex hydrocarbons, exhibits interesting combustion characteristics such as cool flames, negative temperature coefficient regions [5], two-stage autoignition, and product formation at low temperatures [6]. Logically, it follows that understanding butane will give insight to other more complex hydrocarbons. To date, there have been many studies investigating the behavior of *n*-butane oxidation [5–21], while only a few examine isobutane [5,8]. It is important to investigate butane because its two isomers have been shown to have different combustion characteristics [4,5,8,21]. Previous investigations have utilized many different techniques such as shock tubes [14], rapid compression machines (RCMs) [5,6,10,17], spark ignition engines [11], jet stirred reactors [12], and homogeneous charge compression engines [13]. In general, there is a lack of data for blends of the two isomers, particularly at pressures of interest to gas turbines and with undiluted fuel-air mixtures.

In the present study, shock-tube experiments have been performed to determine ignition delay times over a wide range of conditions for 50/50 *n*-/isobutane blends in theoretical air ($O_2 + 3.76N_2$), as seen in Table 1. The range of conditions includes equivalence ratios of $0.3 \leq \phi \leq 2.0$, where the equivalence ratio is the mass-based fuel-to-oxidizer ratio to the stoichiometric fuel-to-oxidizer ratio, target pressures of around $1 \leq P$ (atm) ≤ 21, and temperatures of 1056–1598 K. The results from this work are important to validate chemistry models.

A discussion on the chemical kinetics modeling follows, along with a comparison of the model to experimental results. Additionally, details of the experimental setup and a discussion concerning the approach used to determine ignition delay times are provided

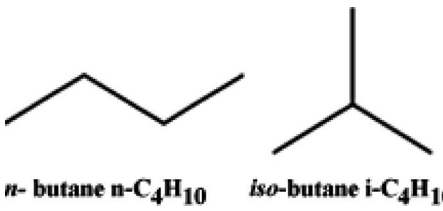

Fig. 1 ***n*-butane and isobutane chemical structures. Normal butane carbon atoms are arranged in one row, while isobutane has a carbon atom in the middle [4].**

Contributed by the International Gas Turbine Institute of ASME for publication in the JOURNAL OF ENGINEERING FOR GAS TURBINES AND POWER. Manuscript received March 26, 2009; final manuscript received April 7, 2009; published online March 4, 2010. Review conducted by Dilip R. Ballal. Paper presented at the ASME Gas Turbine Technical Congress and Exposition, Orlando, FL, June 8–12, 2009.

Table 1 Mixture compositions in percent volume

Mixture	ϕ	n-C_4H_{10} (%)	iso-C_4H_{10} (%)
1	0.3	50	50
2	0.5	50	50
3	1.0	50	50
4	2.0	50	50

in the following sections. Lastly, a thorough discussion of the results is provided as well as results from developed correlations. A sensitivity analysis is also presented to give insight to the important reactions for ignition under varying conditions.

2 Chemical Kinetics Model

The chemical kinetics mechanism was developed, and simulations were performed using the HCT (Hydrodynamics, Chemistry, and Transport) program [22]. The detailed chemical kinetics model is based on that used to describe methane/propane [23] and methane/ethane/propane mixtures [24], but some changes have been made, and these are discussed here. The thermochemistry of a number of species has been taken from the CHEMKIN thermochemistry library [25] or recalculated using THERM [26] with updated groups based on the work of Lay et al. [27] and Sumathi and Green [28] (Table 2). In the mechanism, reactions obey the thermodynamic equilibrium, and thus changes in thermochemistry have led to changes in rate constants of reactions involving these species.

Figure 2 shows how well the model performs over wide ranges

Table 2 Sample of thermochemistry data for species that were changed for the present mechanism, where H_f^0 is the standard heat of formation, S_f^0 is the entropy, and C_p is specific heat under constant pressure

SPECIES	H_f^0 at 298 K (kcal mol^{-1})	S_f^0 at 298 K (cal K^{-1} mol^{-1})	C_p (cal K^{-1} mol^{-1}) 300	400	500	600	800	1000	1500
CH_2[a]	92.49	46.72	8.25	8.55	8.88	9.23	9.93	10.57	11.74
C_2[a]	171.31	37.76	4.98	4.98	4.97	4.97	4.97	4.97	4.97
CH_2CO[a]	−12.40	57.79	12.43	14.17	15.67	16.91	18.79	20.24	22.44
HCCO[a]	42.45	60.74	12.65	13.47	14.23	14.92	16.07	16.83	17.98
HCCOH[a]	20.43	58.71	13.22	14.78	16.16	17.35	19.15	20.30	22.29
C_2H_5CHO[b]	−45.36	72.75	19.82	23.24	26.77	30.28	36.85	42.35	50.07
C_2H_5CO[b]	−7.96	73.87	19.31	21.77	24.62	27.65	33.64	38.76	45.41
HO_2CH_2OCHO[b]	−110.29	90.89	25.72	30.04	33.61	36.54	40.88	43.74	47.49
$HOCH_2OCO$[b]	−82.59	81.62	19.83	22.28	24.60	26.74	30.41	33.18	36.77
CH_3OCHO[b]	−85.68	68.10	15.62	18.97	22.09	24.95	29.73	33.22	37.35
CH_3OCO[b]	−39.37	68.94	14.74	17.57	20.20	22.60	26.56	29.38	32.53
CH_2OCHO[b]	−37.42	70.63	14.64	17.57	20.24	22.62	26.52	29.28	32.46
C_3H_8[b]	−25.06	64.29	17.90	22.77	27.08	30.89	37.16	41.95	49.33
n-C_3H_7[b]	23.94	69.08	17.13	21.39	25.17	28.50	34.00	38.20	44.68
iso-C_3H_7[b]	21.29	68.80	16.56	20.48	24.11	27.42	33.12	37.58	44.33
C_3H_6[b]	4.87	63.82	15.45	19.32	22.74	25.75	30.72	34.51	40.34
C_3H_5-a[b]	40.97	60.69	14.88	18.70	21.94	24.68	28.96	32.07	36.88
C_3H_5-t[b]	61.78	65.63	15.09	18.09	20.80	23.24	27.37	30.59	35.58
C_3H_5-s[b]	63.98	65.21	15.26	18.51	21.36	23.85	27.92	31.01	35.82
C_3H_4-a[b]	47.64	57.95	14.25	16.97	19.46	21.71	25.45	28.20	32.06
C_3H_4-p[b]	45.77	58.90	14.51	17.06	19.40	21.54	25.16	27.90	31.79
C_3H_3[b]	83.05	61.49	15.84	17.74	19.47	21.01	23.43	25.00	27.55
C_3H_6OOH2-2[b]	1.00	88.11	26.02	31.08	35.29	38.78	44.14	47.97	54.08
$C_3H_5$1-2,3OOH[b]	−20.00	104.98	33.45	39.90	45.21	49.55	56.01	60.37	66.48
$C_3H_5$2-1,3OOH[b]	−17.98	103.80	33.05	39.02	44.08	48.35	54.95	59.59	66.07
C_2H_3OOH[b]	−7.59	72.50	18.43	22.06	25.07	27.55	31.25	33.75	37.25
C_4H_{10}[b]	−30.04	73.71	23.34	29.68	35.27	40.17	48.21	54.27	63.52
pC_4H_9[b]	18.96	78.50	22.57	28.30	33.36	37.79	45.05	50.53	58.86
sC_4H_9[b]	16.31	79.52	21.81	27.37	32.37	36.84	44.27	49.92	58.31
C_4H_8-1[b]	0.07	73.51	20.62	26.22	31.06	35.25	41.98	47.00	54.71
C_4H_8-2[b]	−2.78	71.03	20.67	25.84	30.45	34.53	41.29	46.45	54.32
C_4H_8OH-1[b]	−19.71	90.39	24.82	30.85	36.15	40.80	48.37	54.03	62.47
C_4H_8OH-2[b]	−24.08	88.39	25.43	31.55	36.89	41.53	49.02	54.58	63.00
$C_2H_3COCH_3$[b]	−30.40	78.20	21.23	26.36	30.77	34.55	40.53	44.88	51.30
iso-C_4H_{10}[b]	−32.07	70.11	23.33	29.79	35.44	40.38	48.41	54.49	63.86
iso-C_4H_9[b]	16.93	75.21	22.54	28.40	33.53	37.99	45.26	50.74	59.21
tC_4H_9[b]	12.33	75.35	22.45	27.38	31.98	36.22	43.59	49.46	58.47
iso-C_4H_8[b]	−4.21	71.37	21.58	26.74	31.30	35.31	41.90	46.91	54.64
iso-C_4H_7[b]	31.89	69.62	20.99	26.11	30.47	34.20	40.10	44.44	51.16
tC_3H_6OH[b]	−24.40	76.94	20.50	24.97	28.79	32.06	37.24	41.06	47.12
$tC_3H_6O_2CHO$[b]	−39.73	93.50	30.47	36.84	42.27	46.88	54.07	59.18	66.46
$tC_3H_6O_2HCO$[b]	−38.93	94.40	31.74	38.35	43.91	48.56	55.63	60.46	66.91
iso-$C_3H_5O_2HCHO$[b]	−26.83	96.70	31.82	38.41	43.96	48.59	55.63	60.44	66.90

[a]Kee et al. [25].
[b]Ritter and Bozzelli [26], Lay et al. [27], and Sumathi and Green [28].

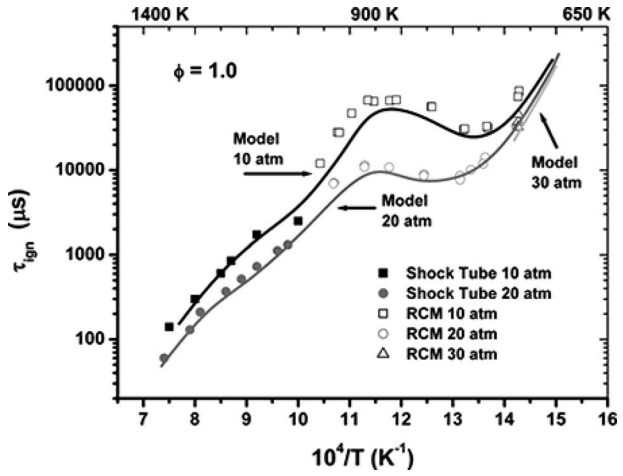

Fig. 2 Validation of model for 100% *n*-butane in air (ϕ=1) over a wide range of conditions. Points are experimental results; lines are model simulations. Data are from Ref. [29].

of temperatures (650–1400 K) and pressures (10–30 atm) for pure *n*-butane/air mixtures. The data shown in Fig. 2 were taken from a recent study by the authors, presented elsewhere [29]. A complete listing of the detailed kinetic mechanism, together with thermochemical parameters and transport data, is available on the NUI Galway combustion chemistry website.[1]

3 Experiment

As mentioned above, shock-tube experiments were performed over a wide range of conditions to better understand the ignition behavior of various 50/50 blends of *n*-/isobutane. The experiments were performed using two separate shock tubes as described later in this section. Pressure traces from the experiment were analyzed to determine ignition time. The ignition-delay data were then used to help validate the chemical kinetics mechanism.

3.1 Apparatus and Procedure. Two shock-tube facilities capable of achieving the high pressures and temperatures needed for the present study are described in this section. Both facilities measure the incident-shock velocity at the test region to determine the overall conditions behind the reflected shock by way of one-dimensional shock relations. The incident-shock measurement is facilitated by five pressure transducers (PCB 113) set in series along the side of the shock tube, which feed signals to four Fluke PM 6666 timer counter boxes, which in turn are used to extrapolate the incident-shock velocity directly to the end wall.

The first facility, described in greater detail by Petersen et al. [30], used in generating all of the data in the intermediate- to high-pressure region, has a driven section length of 10.7 m with a circular profile internal diameter of 16.2 cm. The driver section of this first facility is 3.5 m in length and has a smaller internal diameter of 7.62 cm, which is then expanded through a nozzle cone to the driven diameter directly after the diaphragm location. The second facility, presented by Aul et al. [31], has a driven section length and inner diameter dimensions of 4.72 m and 15.24 cm, respectively, and a driver section length and an inner diameter of 4.93 m and 7.62 cm, respectively. A schematic of the second facility is shown in Fig. 3. Both facilities are constructed entirely of stainless steel 304, which is wholly inert to the test gases used in this study.

Ignition-delay-time measurements are determined from the highly exothermic pressure rise present during reaction via PCB 134A and Kistler 603B1 pressure transducers located at the sidewall and end wall of each shock-tube facility. Measurements of the emission of OH^* chemiluminescence are made at both the sidewall and end wall locations through CaF_2 windows and are focused onto a 307 ± 5 nm bandpass filter in sequence with a Hamamatsu 1P21 photomultiplier tube in a home-made housing. Each of the data signals is processed through a 14 bit GageScope digital oscilloscope board with sampling rates of 1 MHz or greater per channel.

3.2 Ignition Time Definition. The ignition time is measured from the end wall as the sudden rise in pressure behind the reflected-shock wave. For these real fuel-air mixtures, a sharp rise is seen in the pressure trace during ignition, which also coincides with the onset of OH^* emission, as shown in Fig. 4(*a*). The end wall pressure trace was used quantitatively to determine ignition time, while the end wall emission trace was used qualitatively to verify the ignition event. For the mixtures analyzed in this work, no significant pressure rises before ignition were observed, even under colder temperatures and longer test times, as seen in Fig. 4(*a*). Figure 4(*b*) shows the pressure and emission traces for a different temperature and stoichiometry and is representative of all test cases. No pre-ignition pressure rises, such as those sometimes seen in lower-temperature, higher-pressure experiments,

[1]http://c3.nuigalway.ie/butane.html

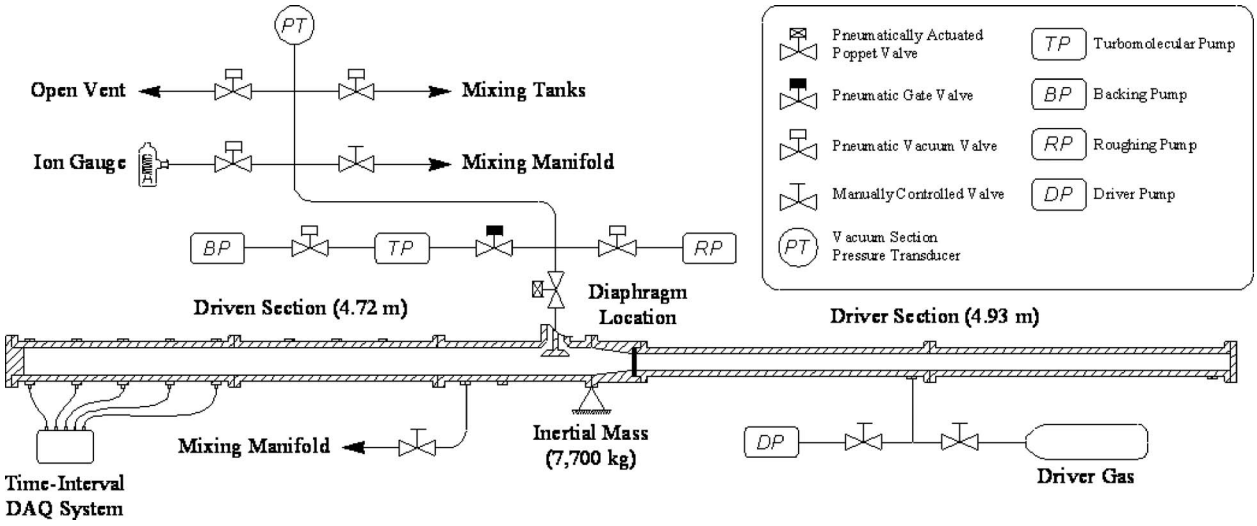

Fig. 3 Schematic of shock-tube facility presented in Aul et al. [31]

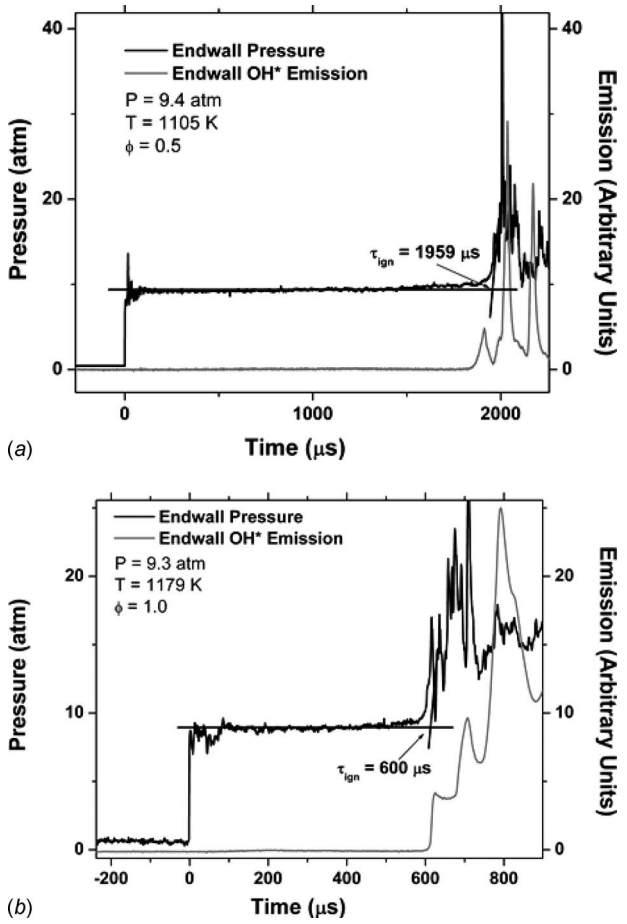

Fig. 4 Typical end wall pressure and emission traces used to determine ignition delay time. No early reaction leading to accelerated main ignition is seen in either the pressure or OH* traces. (*a*) Long test time example: T=1105 K and τ_{ign} =1959 μs. (*b*) Typical test time example: T=1179 K and τ_{ign} =600 μs.

were observed in any of the data presented herein. Such early pressure increases have been linked to faster-than-expected ignition events in some studies [32].

4 Results

The experimental results for the entire range of conditions are provided in Table 3, where the definition of ignition delay time for each case was defined as the inflection point between the test pressure achieved after compressing the mixture and the steep rise in pressure at the time of ignition, as described above.

The experimental data for all four mixtures are plotted in Figs. 5–8 on Arrhenius-type plots that give the ignition delay time on a log scale as a function of the reciprocal reflected-shock temperature. Predicted ignition times from the C4 mechanism are shown on each plot as well. The effect of temperature on the ignition times can be discerned from the data. For temperatures above about 1175 K, the ignition trend becomes more linear, and the slope is steeper. This trend is noticeable for all the mixtures herein. In general, the model is in excellent agreement with the measured ignition delay times, particularly at the higher pressures.

There is a small but noticeable ignition delay time uncertainty that is apparent for measurements lower than 200 μs and has been statistically averaged throughout the collection of data to be ± 8 μs. This uncertainty in time is the result of inherent uncertainties in selecting the specific pressure and/or emission features at the time of the ignition event and also in the repeatability of the

Table 3 Shock-tube ignition-delay-time data for 50/50 *n*-/isobutane mixtures in air

T (K)	P (atm)	τ_{ign} (μs)	ϕ
1354	1.9	166	0.3
1321	2.0	318	
1282	2.0	511	
1255	2.0	725	
1248	2.0	895	
1253	8.6	335	
1151	9.1	1396	
1307	7.9	169	
1102	8.9	2380	
1190	8.5	878	
1266	17.7	223	
1211	18.9	421	
1148	19.5	804	
1099	19.9	1287	
1362	16.9	79	
1383	1.7	130	0.5
1307	1.7	410	
1282	1.9	650	
1263	1.9	973	
1235	1.8	1404	
1363	1.8	199	
1409	1.7	111	
1105	9.4	1959	
1147	8.9	1292	
1239	8.2	444	
1321	7.6	164	
1195	8.6	746	
1323	16.9	89	
1240	17.9	247	
1167	18.5	543	
1115	19.5	846	
1079	20.3	1191	
1406	16.3	42	
1278	1.9	773	1.0
1266	1.8	1045	
1303	1.8	714	
1336	1.8	469	
1355	1.8	380	
1350	1.8	395	
1274	1.9	1053	
1179	9.3	600	
1096	9.3	1662	
1258	7.9	318	
1366	7.1	123	
1111	8.8	1652	
1178	9.3	812	
1220	18.3	266	
1158	19.4	441	
1099	20.0	727	
1062	21.0	987	
1297	16.9	129	
1407	15.4	48	
1300	1.7	784	2.0
1368	1.6	403	
1445	1.5	178	
1517	1.3	115	
1262	1.7	1449	
1194	8.1	637	
1119	8.7	1369	
1076	9.2	2030	
1266	7.4	369	
1361	6.9	165	
1421	6.3	100	
1119	19.1	488	
1056	19.1	871	
1182	18.6	317	
1259	17.4	187	
1317	16.0	107	

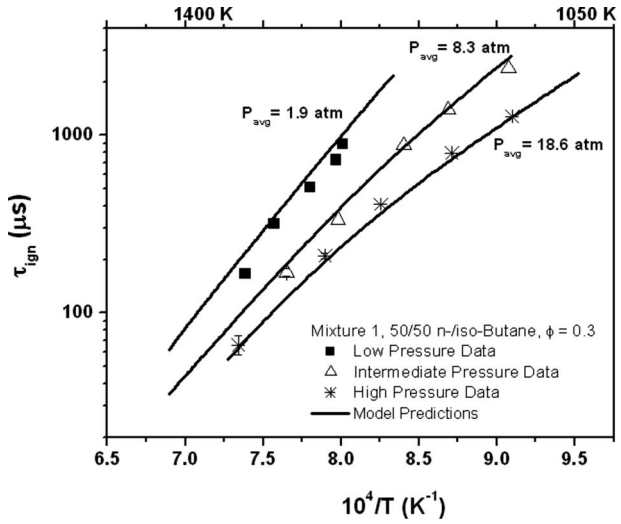

Fig. 5 Ignition-delay-time data compared with model results for mixture 1: 50% n-C_4H_{10} and 50% iso-C_4H_{10} at ϕ=0.3

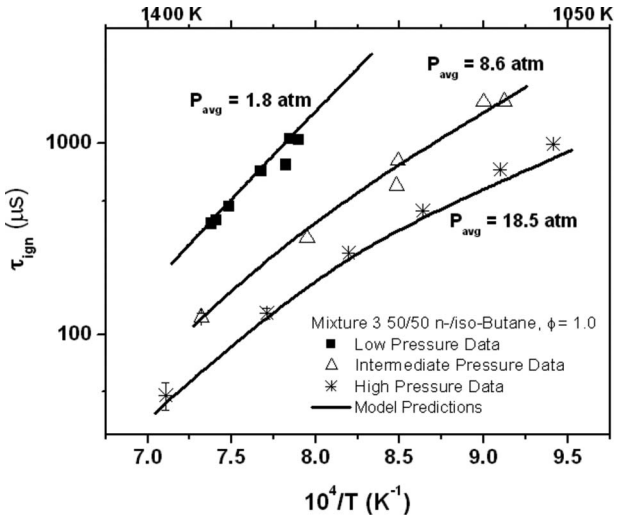

Fig. 7 Ignition-delay-time data compared with model results for mixture 3: 50% n-C_4H_{10} and 50% iso-C_4H_{10} at ϕ=1.0

ignition event itself from test to test. This variation is almost insignificant for longer ignition times and is thus only shown in error bars for the faster ignition results.

5 Discussion

The experimental results are in agreement with the present C4 mechanism over the entire range of temperatures, pressures, and stoichiometries, as seen in Figs. 5–8. Any slight disagreement that does exist between the model and the data occurs at the lower pressure (Fig. 8), where the model overpredicts the ignition at higher temperatures. Since the model is validated over the conditions of the experiment, it can be used to explore the effect of mixtures and conditions not directly measured in the experiment.

Figure 9 compares the results from the model for the cases of 100% n-butane, 0% isobutane all the way to the case of 0% n-butane, 100% isobutane in 25% increments for various stoichiometries (ϕ=0.3, 0.5, 1.0, and 2.0) at P=8 atm. An interesting effect is seen at fuel lean conditions (Figs. 9(a) and 9(b)), where there is little variation in ignition times between 100% n-butane and 100% isobutane. There becomes a clear distinction in ignition times of the two different isomers when the fuel blend is stoichiometric, as seen in Fig. 9(c). This difference becomes even more exaggerated under fuel rich conditions, where in Fig. 9(d) n-butane is seen to ignite significantly faster than isobutane. A sensitivity analysis was performed to further examine this effect and is presented later in this section.

In other ongoing work, the authors have performed an extensive series of rapid compression and shock-tube ignition-delay-time experiments for the cases of 100% isobutane as well as 100% n-butane [29]. This work agrees with the predicted results shown in Fig. 9 and was also mentioned above with regard to Fig. 3. Correlations have been developed from the experimental results to predict ignition delay times. Each correlation determines ignition times for a given temperature, pressure, and amount of n-butane and isobutane. The correlations help to give an understanding of the complex chemistry by providing simplified physical relationships. Following traditional hydrocarbon fuel ignition time behavior, it is seen that the ignition time is exponentially dependent on the inverse temperature and directly dependent on the mixture concentration to some power. The basic form of the correlation is as follows:

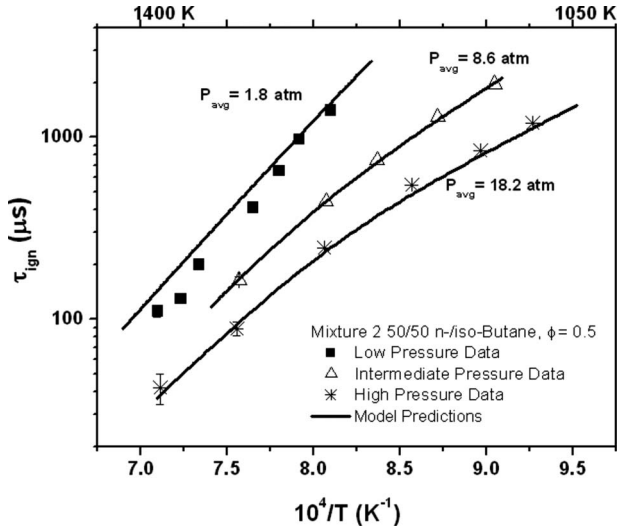

Fig. 6 Ignition-delay-time data compared with model results for mixture 2: 50% n-C_4H_{10} and 50% iso-C_4H_{10} at ϕ=0.5

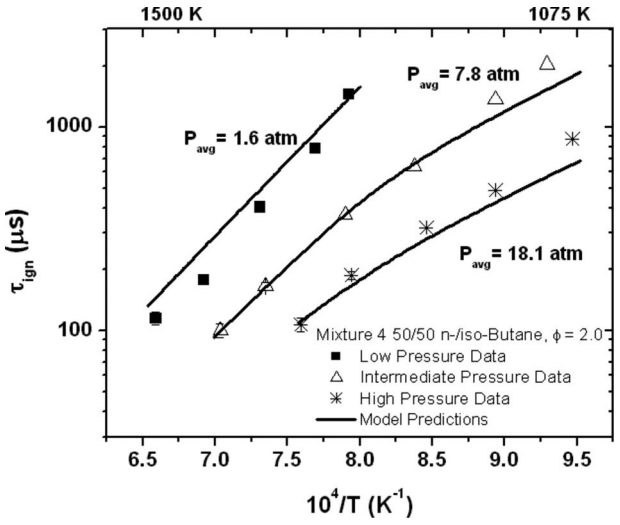

Fig. 8 Ignition-delay-time data compared with model results for mixture 4: 50% n-C_4H_{10} and 50% iso-C_4H_{10} at ϕ=2.0

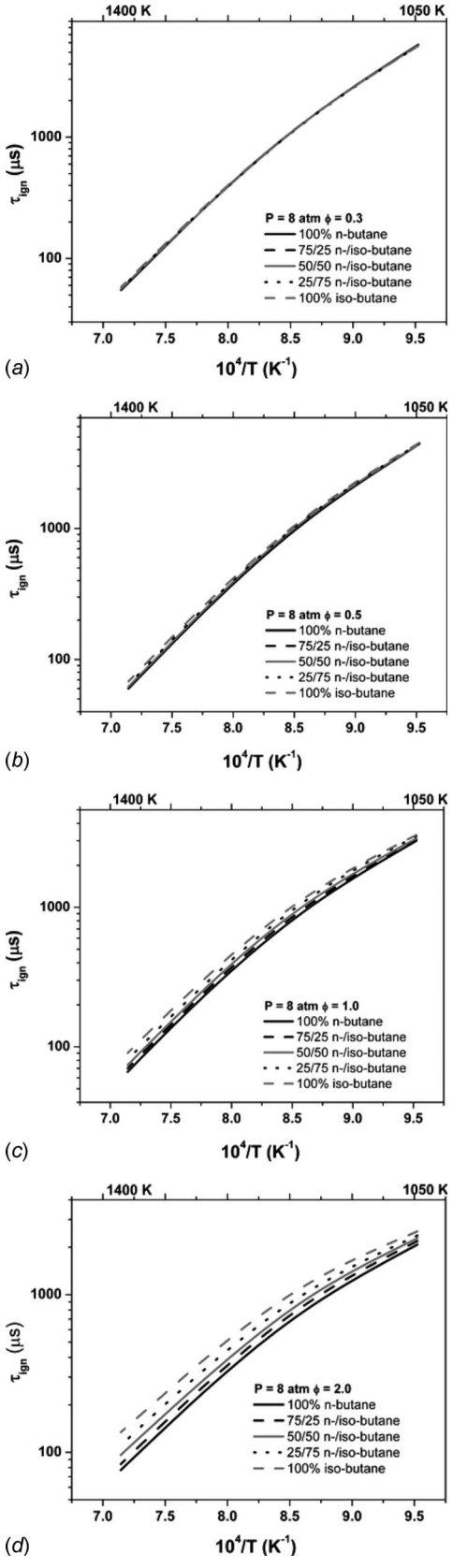

Fig. 9 Ignition delay times obtained from the mechanism are plotted against inverse temperature at 8 atm for a wide range of stoichiometry. Fuel lean conditions show similar ignition times for *n*-C_4H_{10} and iso-C_4H_{10}; however, under stoichiometric and fuel rich conditions, *n*-C_4H_{10} and iso-C_4H_{10} have significantly different ignition times. (*a*) ϕ=0.3, (*b*) ϕ=0.5, (*c*) ϕ=1.0, and (*d*) ϕ=2.0.

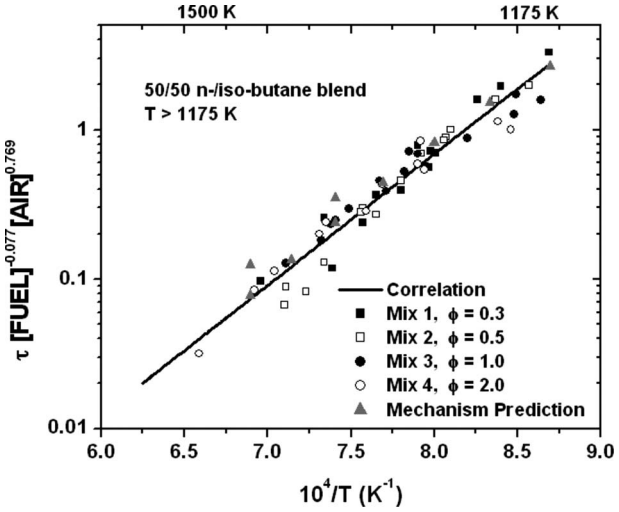

Fig. 10 High-temperature correlation from Eq. (2). Experimental data, correlation results, and mechanism predictions plotted against inverse temperature show good agreement for high temperatures (τ in μs; [fuel] and [air] in mol/cm^3).

$$\tau_{\text{ign}} = A[\text{fuel}]^x[\text{air}]^y \exp\left(\frac{E}{RT}\right) \tag{1}$$

where τ_{ign} is the ignition delay time or kinetic time in μs; fuel is 50/50 *n*-C_4H_{10} plus iso-C_4H_{10} in mol/cm^3; air is also in mol/cm^3; E, A, x, and y are constants. The constant E is commonly referred to as an ignition activation energy, which is in kcal/mol, and R is the ideal gas constant in kcal/mol K units. As noted above, there is a shift in temperature dependence between the higher-temperature and lower-temperature data, so two correlations were found to best fit the data.

The first correlation was developed for temperatures greater than 1175 K (Eq. (2)). When using the data to obtain the correlation, data that were close to 1175 K were used in both the high- and low-temperature correlations, so that the correlations will overlap,

$$\tau_{\text{ign}} = 6.734 \times 10^{-8}[\text{fuel}]^{0.077}[\text{air}]^{-0.769} \exp(40.1/RT) \tag{2}$$

The pressure dependence of ignition delay can be estimated as the pressure raised the sum of the exponents of the fuel and air terms since the fuel and air concentrations both depend linearly on the

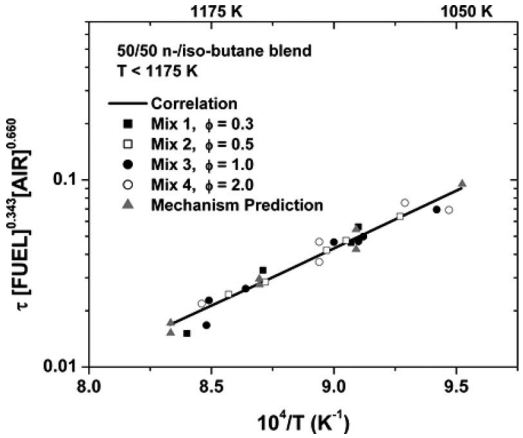

Fig. 11 Low-temperature correlation of Eq. (3). A shallower slope is seen for the lower temperature experimental data, correlation, and mechanism predictions when plotted against inverse temperature (τ in μs; [fuel] and [air] in mol/cm^3).

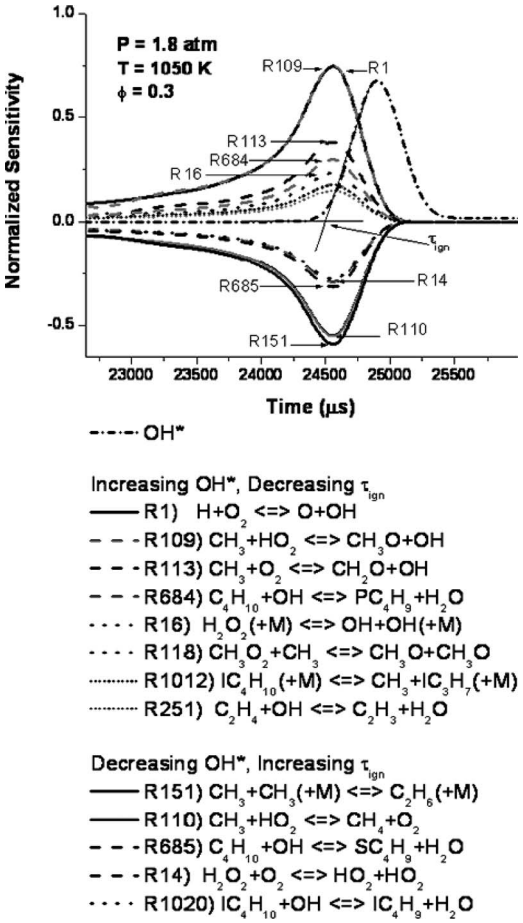

Fig. 12 Sensitivity analysis results from OH* show the most important reactions as a function of time during ignition. Sensitivity results for low pressure (1.8 atm) and low temperature (1050 K).

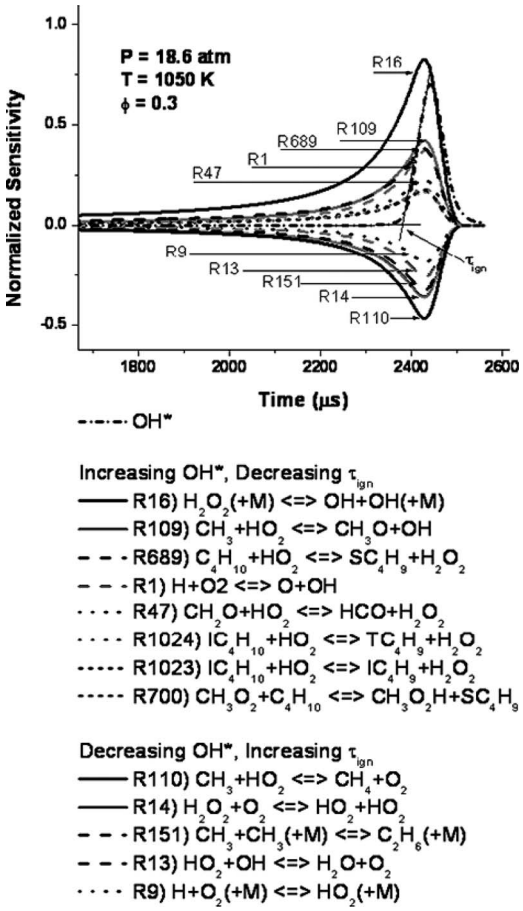

Fig. 13 Sensitivity analysis results from OH* show the most important reactions as a function of time during ignition. Results shown for high pressure (18.6 atm) and low temperature (1050 K).

pressure. The above equation gives an overall pressure dependency of $P^{-0.69}$. The negative exponents of fuel and air show that ignition will become faster with increasing amounts of fuel and air. Results from the high-temperature correlation compared with the experimental results and mechanism predictions show good agreement, as seen in Fig. 10, with an $R^2=0.93$.

The mechanism was run over the conditions of the experimental range to determine predicted ignition delay times. The results from the mechanism were then compared with the correlation. Figures 10 and 11 show excellent agreement between the predicted results and the correlation for the same range of temperatures, pressures, and equivalence ratios.

In a similar fashion, a low-temperature correlation was developed for temperatures less than 1175 K,

$$\tau_{\text{ign}} = 1.335 \times 10^{-7}[\text{fuel}]^{-0.343}[\text{air}]^{-0.660}\exp\left(\frac{28.0}{RT}\right) \qquad (3)$$

Here, a pressure dependence of $P^{-1.003}$ was seen. Once again, good agreement, $R^2=0.96$, is seen between the correlation, experimental data, and mechanism predictions, as shown in Fig. 11.

The activation energy, E, for the high-temperature correlation (40.1 kcal/mol) is larger than that of the lower-temperature correlation (28.0 kcal/mol). This difference corresponds to a steeper slope when plotted against an inverse temperature, as seen in Figs. 10 and 11.

To gain further insight to the chemical processes occurring during ignition, a sensitivity analysis was performed. A range of stoichiometries from lean to rich for 50/50 *n*-/isobutane mixtures was investigated in the sensitivity study. Within the mixtures, high (1400 K) and low (1050 K) temperatures were chosen as well as high (18.6 atm) and low (1.8 atm) pressures. Using CHEMKIN [33], a sensitivity analysis was performed on the species OH*. Although this is not the same as performing a direct ignition-delay sensitivity, it is qualitatively similar since there is a sudden buildup of the radical OH* at ignition and because OH* chemiluminescence is a marker of ignition in the experiments. The majority of the key reactions that mostly affect ignition will show up in the excited hydroxyl radical sensitivity. It should be noted that reactions that have a positive or increasing effect on OH*, which is a highly reactive species, lead to decreasing ignition time, while reactions that have a negative or decreasing effect on OH* will increase ignition time.

Figures 12 and 13 show normalized sensitivities for the top reactions at a given condition versus time. Figure 12 provides the low-pressure, low-temperature case, while Fig. 13 shows the high-pressure, low-temperature results, both for fuel lean conditions. The OH* mole fraction is also shown on the plot and used to determine ignition. At the time of ignition, the most important reactions are listed. The reaction numbering scheme used in this paper follows that used in the C4 mechanism.

The OH* sensitivity analysis for the fuel lean cases revealed that the top reactions for all cases are well known reactions from the methane and hydrogen mechanisms. Under most conditions, the chain branching reaction R1 ($H+O_2=OH+O$), which helps to speed up ignition, is the most important reaction. At low pressures (both at high and low temperatures), the most influential reactions in speeding up ignition time other than R1 were R109,

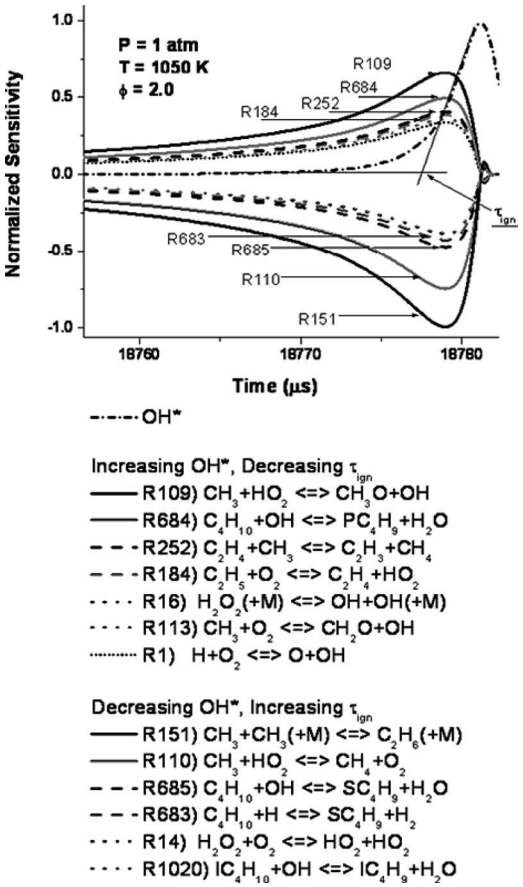

Fig. 14 Sensitivity analysis results from OH* show the most important reactions as a function of time during ignition. Sensitivity results show that the key reactions for fuel rich conditions are different from those reactions for fuel lean conditions at low pressure (1 atm) and low temperature (1050 K).

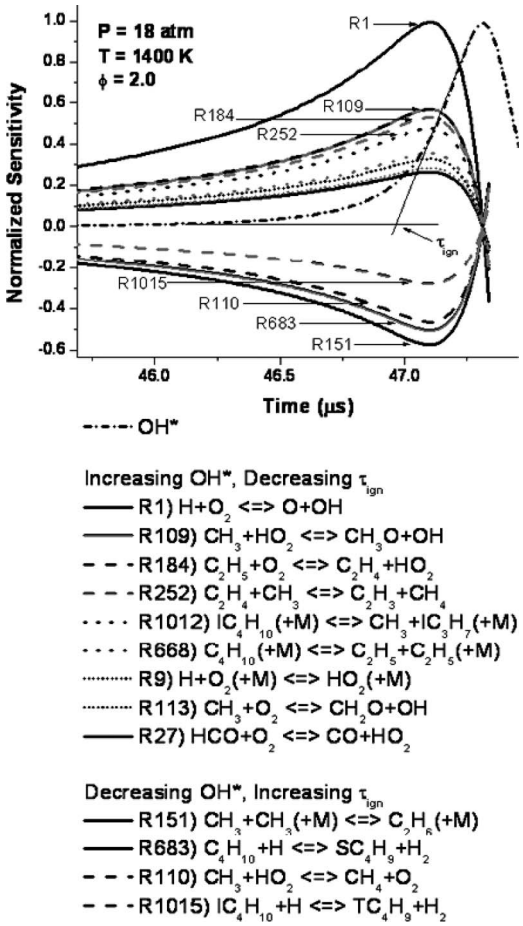

Fig. 15 Sensitivity analysis results from OH* show the most important reactions as a function of time during ignition. Sensitivity analysis results show that the important reactions for fuel rich conditions are different from those reactions for fuel lean conditions at high pressure (18 atm) and high temperature (1400 K).

$$CH_3 + HO_2 = CH_3O + OH$$

and R113,

$$CH_3 + O_2 = CH_2O + OH$$

At high pressures and low temperatures (Fig. 13), R1, while still influential, is not the most important reaction in accelerating ignition. Of more importance at these conditions is reaction 16, the hydrogen peroxide decomposition reaction that forms two of the highly reactive radical OH,

$$H_2O_2 + M = OH + OH + M$$

When looking at high pressures and low temperatures, peroxide reactions become most important, as expected.

Interestingly, the only C4 reactions that show up as being important for lean ignition at the conditions of interest herein are the hydrogen abstraction reactions of the butanes with OH at the lower pressures (R684, R685, and R1020 in Fig. 12) and with HO_2 at the higher pressures (R689, R1023, and R1024 in Fig. 13). Isobutane pyrolysis also has some importance at the lower pressure (R1012, Fig. 12).

As previously mentioned, the composition of the fuel blend has an increasingly greater effect on the ignition time at fuel rich conditions than at fuel lean conditions, as seen in Figs. 9(*a*)–9(*d*). A sensitivity analysis on OH* at fuel rich conditions (ϕ=2.0) confirms that the key reactions vary between fuel lean and fuel rich conditions. Figure 14 provides the low-pressure, low-temperature case, while Fig. 15 shows the high-pressure, high-temperature results, both for fuel rich conditions. Figure 14 shows that the most important reactions in speeding up ignition at low pressures and low temperatures are different from those of the fuel lean case (Fig. 12). The oxygen-containing, chain branching reaction, R1, is no longer the most important reaction. Two new reactions show up as being important at these conditions, R252,

$$C_2H_4 + CH_3 = C_2H_3 + CH_4$$

and R184,

$$C_2H_5 + O_2 = C_2H_4 + HO_2$$

These hydrocarbon reactions become more important under fuel rich conditions.

The examination of sensitivity analysis results for fuel rich conditions at high pressure (18 atm) and high temperature (1400 K), as seen in Fig. 15, reveals that some of the most influential reactions on ignition time are different from the reactions that were most important at fuel lean conditions. For high pressures and high temperatures, the two most important reactions for decreasing ignition time, R1 and R109, are the most important reactions for both fuel lean and rich conditions. However, the next two most important reactions are different. At fuel rich conditions, the hydrocarbon reactions R184 and R252 prove to be important. Additionally, the butane decomposition reaction R668 becomes influential in accelerating ignition,

$$C_4H_{10}(+M) = C_2H_5 + C_2H_5(+M)$$

While many of the same reactions that increase ignition time show up for both fuel lean and fuel rich conditions, the influence of the most significant reactions changes.

6 Conclusion

Shock-tube experiments have been performed over a wide range of conditions to validate the chemical kinetics mechanism for a blend of 50/50 *n*-/isobutane in air at pressures up to approximately 20 atm. This study marks the first of its kind to perform such an extensive investigation into this isomer fuel blend. A very good agreement has been demonstrated between the chemical kinetics model developed herein and the data. Additionally, useful correlations were developed to gain insight on the fundamental behavior of the system including important physical relationships such as the effect of stoichiometry on ignition times for different fuel blends and the pressure dependence of the ignition delay time. At lean conditions, the butane type has little effect on ignition time, whereas at stoichiometric and rich conditions, differences between *n*- and isobutane become apparent.

Acknowledgment

This work was supported primarily by Rolls-Royce Canada. Additional support came from the National Science Foundation (Grant No. CBET-0832561) and from The Aerospace Corporation.

References

[1] Richards, G. A., McMillian, M. M., Gemmen, R. S., Rogers, W. A., and Cully, S. R., 2001, "Issues for Low-Emission, Fuel Flexible Power Systems," Prog. Energy Combust. Sci., **27**, pp. 141–169.

[2] Lieuwen, T., McDonell, V., Petersen, E., and Santavicca, D., 2008, "Fuel Flexibility Influences on Premixed Combustor Blowout, Flashback, Autoignition and Stability," ASME J. Eng. Gas Turbines Power, **130**, p. 011506.

[3] Von Richer, V., 1947, *Chemistry of the Carbon Compounds; Or, Organic Chemistry*, Blakiston, New York, p. 74.

[4] Ogura, T., Nagumo, Y., Miyoshi, A., and Koshi, M., 2007, "Chemical Kinetic Mechanism for High Temperature Oxidation of Butane Isomers," Energy Fuels, **21**, pp. 130–135.

[5] Griffiths, J. F., Halford-Maw, P. A., and Rose, D. J., 1993, "Fundamental Features of Hydrocarbon Autoignition in a Rapid Compression Machine," Combust. Flame, **95**, pp. 291–306.

[6] Minetti, R., Ribaucour, M., Carlier, M., Fittschen, C., and Sochet, L. R., 1994, "Experimental and Modeling Study of Oxidation and Autoignition of Butane at High Pressure," Combust. Flame, **96**, pp. 201–211.

[7] Pitz, W. J., and Westbrook, C. K., 1986, "Chemical Kinetics of the High Pressure Oxidation of *n*-Butane and Its Relation to Engine Knock," Combust. Flame, **63**, pp. 113–133.

[8] Fotache, C. G., Wang, H., and Law, C. K., 1999, "Ignition of Ethane, Propane, and Butane in Counter Flow Jets of Cold Fuel Versus Hot Air Under Variable Pressures," Combust. Flame, **117**, pp. 777–794.

[9] Chandraratna, M. R., and Griffiths, J. F., 1994, "Pressure and Concentration Dependence of the Autoignition Temperature for Normal Butane+Air Mixtures in a Closed Vessel," Combust. Flame, **99**, pp. 626–634.

[10] Kojima, S., 1994, "Detailed Modeling of *n*-Butane Autoignition Chemistry," Combust. Flame, **99**, pp. 87–136.

[11] Smith, J. R., Green, R. M., Westbrook, C. K., and Pitz, W. J., 1984, "Experimental and Modeling Study of Engine Knock," 20th International Symposium on Combustion, The Combustion Institute, Pittsburgh, p. 91.

[12] Proudler, V. K., Cederbalk, P., Horowitz, A., Hughes, K. J., and Pilling, M. J., 1991, "Oscillatory Ignitions and Cool Flames in the Oxidation of Butane in a Jet-Stirred Reactor," Philos. Trans. R. Soc. London, Ser. A, **337**(1646), pp. 211–221.

[13] Yudai, Y., and Norimasa, I., 2003, "Numerical Analysis of Autoignition and Combustion of *n*-Butane and Air Mixtures in Homogeneous-Charge Compression-Ignition Engine Using Elementary Reactions," JSME Int. J., Ser. B, **46**, pp. 52–59.

[14] Burcat, A., Scheller, K., and Lifshitz, A., 1971, "Shock-Tube Investigation of Comparative Ignition Delay Times for C1-C5 Alkanes," Combust. Flame, **16**, pp. 29–33.

[15] Buda, F., Bounaceur, R., Warth, V., Glaude, P. A., Fournet, R., and Battin-Leclerc, F., 2005, "Progress Toward a Unified Detailed Kinetic Model for the Autoignition of Alkanes From C4 to C10 Between 600 and 1200 K," Combust. Flame, **142**, pp. 170–186.

[16] Wilk, R. D., Pitz, W. J., Westbrook, C. K., Addagarla, S., Miller, D. L., Cernansky, N. P., and Green, R. M., 1990, "Combustion of *n*-Butane and Iso-Butane in an Internal Combustion Engine: A Comparison of Experimental and Modeling Results," Sym. (Int.) Combust., [Proc.], **23**, pp. 1047–1056.

[17] Kojima, S., and Suzuoki, T., 1993, "Autoignition-Delay Measurement Over Lean to Rich Mixtures of *n*-Butane/Air Under Swirl Conditions," Combust. Flame, **92**, pp. 254–265.

[18] Griffiths, J. F., and Nimmo, W., 1985, "Spontaneous Ignition and Engine Knock Under Rapid Compression," Combust. Flame, **60**, pp. 215–218.

[19] Pekalski, A. A., Terli, E., Zevenbergen, J. F., Lemkowitz, S. M., and Pasman, H. J., 2005, "Influence of the Ignition Delay Time on the Explosion Parameters of Hydrocarbon-Air-Oxygen Mixtures at Elevated Pressure and Temperature," Proc. Combust. Inst., **30**, pp. 1933–1969.

[20] Marengo, S., Comotti, P., and Galli, G., 2003, "New Insight Into the Role of Gas Phase Reaction in the Partial Oxidation of Butane," Catal. Today, **81**, pp. 205–213.

[21] Morley, C., 1987, "A Fundamentally Based Correlation Between Alkane Structure and Octane Number," Combust. Sci. Technol., **55**, pp. 115–123.

[22] Lund, C. M., and Chase, L., 1995, "HCT-A General Computer Program for Calculating Time-Dependent Phenomena Involving One-Dimensional Hydrodynamics, Transport, and Detailed Chemical Kinetics," Lawrence Livermore National Laboratory, Report No. UCRL-52504.

[23] Healy, D., Curran, H. J., Dooley, S., Simmie, J. M., Kalitan, D. M., Petersen, E. L., and Bourque, G., 2008, "Methane/Propane Mixture Oxidation at High Pressures and at High, Intermediate and Low Temperatures," Combust. Flame, **155**, pp. 451–461.

[24] Healy, D., Curran, H. J., Simmie, J. M., Kalitan, D. M., Zinner, C. M., Barrett, A. B., Petersen, E. L., and Bourque, G., 2008, "Methane/Ethane/Propane Mixture Oxidation at High Pressures and at High, Intermediate and Low Temperatures," Combust. Flame, **155**, pp. 441–448.

[25] Kee, R. J., Rupley, F. M., and Miller, J. A., 1987, Sandia National Laboratories, Report No. SAND87-8217.

[26] Ritter, E. R., and Bozzelli, J. W., 1991, "THERM: Thermodynamic Property Estimation for Gas Phase Radicals and Molecules," Int. J. Chem. Kinet., **23**, pp. 767–778.

[27] Lay, T., Bozzelli, J. W., Dean, A. M., and Ritter, E. R., 1995, "Hydrogen Atom Bond Increments for Calculation of Thermodynamic Properties of Hydrocarbon Radical Species," J. Phys. Chem., **99**, pp. 14514–14527.

[28] Sumathi, R., and Green, W. H., Jr., 2003, "Oxygenate, Oxyalkyl, and Alkoxycarbonyl Thermochemistry and Rates for Hydrogen Abstraction From Oxygenates," Phys. Chem. Chem. Phys., **5**, pp. 3402–3417.

[29] Healy, D., Curran, H. J., Petersen, E. L., Aul, C. J., Zinner, C. M., and Bourque, G., 2009, "*n*-Butane: Ignition Delay Measurements at High Pressure and Detailed Chemical Kinetic Simulations," Combust. Flame, submitted.

[30] Petersen, E. L., Rickard, M. J. A., Crofton, M. D., Abbey, E. D., Traum, M. J., and Kalitan, D. M., 2005, "A Facility for Gas- and Condensed-Phase Measurements Behind Shock Waves," Meas. Sci. Technol., **16**, pp. 1716–1729.

[31] Aul, C. J., de Vries, J., and Petersen, E. L., 2007, "New Shock-Tube Facility for Studies in Chemical Kinetics at Engine Conditions," Eastern States Fall Technical Meeting of the Combustion Institute, Charlottesville, VA, Oct. 21–24.

[32] Petersen, E., Lamnaouer, M., de Vries, J., Curran, H., Simmie, J., Fikri, M., Schulz, C., and Bourque, G., 2007, "Discrepancies Between Shock Tube and Rapid Compression Machine Ignition at Low Temperatures and High Pressures," 26th International Symposium on Shock Waves, Göttingen, Germany, Paper No. 0911.

[33] Kee, R. J., Rupley, F. M., Miller, J. A., Coltrin, M. E., Grcar, J. F., Meeks, E., Moffat, H. K., Lutz, A. E., Dixon-Lewis, G., Smooke, M. D., Warnatz, J., Evans, G. H., Larson, R. S., Mitchell, R. E., Petzold, L. R., Reynolds, W. C., Caracotsios, M., Stewart, W. E., Glarborg, P., Wang, C., and Adigun, O., 2000, CHEMKIN Collection, Release 3.6, Reaction Design, Inc., San Diego, CA.